Spacetime as a Quantum Circuit?

Mario Flory

JAGIELLONIAN UNIVERSITY IN KRAKOW

funded by NARODOWE CENTRUM NAUKI
grant 2021/42/E/ST2/00234

Madrid

22.05.2023

Based on 2101.01185 and 2203.08842

The Team:

Spacetime as a quantum circuit

A. Ramesh Chandra,[a] Jan de Boer,[a] Mario Flory,[b,c] Michal P. Heller,[d,1] Sergio Hörtner,[a] and Andrew Rolph[a]

[a] Institute for Theoretical Physics, University of Amsterdam, PO Box 94485, 1090 GL Amsterdam

Cost of holographic path integrals

A. Ramesh Chandra,[a] Jan de Boer,[a] Mario Flory,[b]
Michal P. Heller,[c] Sergio Hörtner,[d] and Andrew Rolph[a]

[a] Institute for Theoretical Physics, University of Amsterdam

See also talk by Andrew later!

Overview

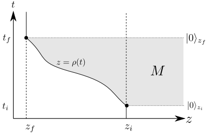

- Introduction
- A first example

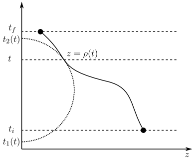

- Kinematic space
- Generic flow equations

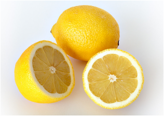

- What does $K^n_m K^m_n - K^2 = 0$ mean?
- Summary

Introduction

Introduction

- One important approach to complexity is *path integral optimization* [Caputa et al. 2017a] [Caputa et al. 2017b].

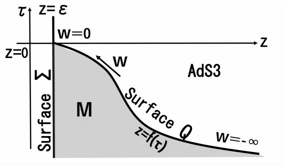

- Further progress came in [Boruch et al. 2021b]:
  - Idea: Compute action between boundary cutoff and bulk surface Q, extremise w.r.t. scale factor of metric of Q.
  - Add tension term T to action on Q $\rightarrow$ plays role of emergent time.
  - This provides *finite cutoff corrections* to Liouville approach beyond $\partial\phi \ll e^{\phi}$.
  - Further work in [Boruch et al. 2021a] [Caputa et al. 2022] [Camargo et al. 2022].
- Around the same time, we were considering a similar setup, leading up to [Chandra et al. 2021].

Basic idea

- Consider a subregion M of Euclidean Poincaré AdS_3.
- Introduce two time-slices $t = t_{i/f}$ corresponding to the ground states $|0\rangle_{z_{i/f}}$ at different values of the radial cutoff.
- The radial boundary is at finite cutoff, $z = \rho(t)$.
- Proposal: Complexity of the circuit that maps between $|0\rangle_{z_{i/f}}$ is given by the gravitational action on M.

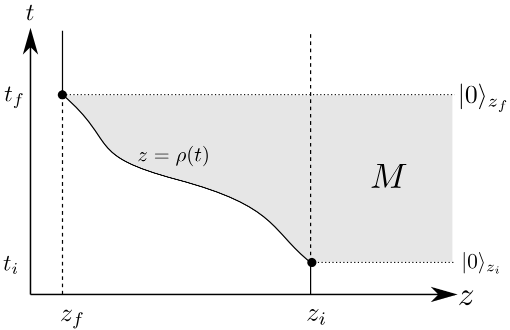

A first example

Simple example - setup

We consider Euclidean AdS, with the curvature scale $l_{AdS} = 1$:

$$ds^2 = \frac{dz^2 + dt^2 + dx^2}{z^2}. \tag{1}$$

Bulk action:

$$I = \frac{1}{\kappa}\int_M d^3x\,\sqrt{G}\,(\mathcal{R}+2) + \frac{2}{\kappa}\int_{\partial M} d^2x\,\sqrt{g}K + I_c. \tag{2}$$

- M is the bulk region bounded by $\rho(t) \le z \le \infty$ and $t_i \le t \le t_f$
- Bulk term
- Surface terms
- Joint terms $I_c = \frac{2}{\kappa}\int dx\sqrt{j}\;\alpha$ [Hartle and Sorkin 1981] [Hayward 1993]

Simple example - boundary surface

We investigate the bulk region M
bounded by $\rho(t) \leq z \leq \infty$ and $t_i \leq t \leq t_f$.

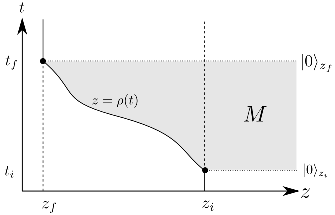

The induced line element on the boundary surface is

$$ds^2 = \frac{(1+\dot{\rho}^2)dt^2 + dx^2}{\rho^2}, \tag{3}$$

hence

$$R = \frac{2(\rho\ddot{\rho} - \dot{\rho}^2(1+\dot{\rho}^2))}{(1+\dot{\rho}^2)^2}, \tag{4}$$

$$K = \frac{\rho\ddot{\rho} + 2(1+\dot{\rho}^2)}{(1+\dot{\rho}^2)^{3/2}}. \tag{5}$$

Simple example - action

We obtain

$$
\begin{aligned}
I &= \frac{-4}{\kappa} \int_M d^2x \int_{z=\rho}^{\infty} \frac{dz}{z^3} + \frac{2}{\kappa} \int_{\partial M} d^2x \, \frac{\rho\ddot{\rho} + 2(1+\dot{\rho}^2)}{\rho^2(1+\dot{\rho}^2)} + I_c[\rho] \\
&= \frac{2V_x}{\kappa} \int_{t_i}^{t_f} dt \, \frac{\rho\ddot{\rho} + (1+\dot{\rho}^2)}{\rho^2(1+\dot{\rho}^2)} + I_c[\rho]
\end{aligned}
\tag{6}
$$

for the on-shell bulk action ($V_x = \int dx$). For the corner term, we also find

$$
I_c = \frac{2V_x}{\kappa} \left(\frac{\pi/2 - \arctan \dot{\rho}(t_f)}{z_f} + \frac{\pi/2 + \arctan \dot{\rho}(t_i)}{z_i} \right). \tag{7}
$$

Integrating by parts, this action can be written only using first derivatives of ρ, yielding

$$
I = \frac{2V_x}{\kappa} \int_{t_i}^{t_f} dt \, \left(\frac{1}{\rho^2} + \frac{\dot{\rho} \arctan \dot{\rho}}{\rho^2} \right) + \frac{\pi V_x}{\kappa} \left(\frac{1}{z_f} + \frac{1}{z_i} \right). \tag{8}
$$

Simple example - action

We obtain

$$
\begin{aligned}
I &= \frac{-4}{\kappa}\int_M d^2x \int_{z=\rho}^{\infty}\frac{dz}{z^3} + \frac{2}{\kappa}\int_{\partial M} d^2x\, \frac{\rho\ddot{\rho}+2(1+\dot{\rho}^2)}{\rho^2(1+\dot{\rho}^2)} + I_c[\rho] \\
&= \frac{2V_x}{\kappa}\int_{t_i}^{t_f} dt\ \boxed{\frac{\rho\ddot{\rho}+(1+\dot{\rho}^2)}{\rho^2(1+\dot{\rho}^2)}} + I_c[\rho] \qquad (6)
\end{aligned}
$$

for the on-shell bulk action ($V_x = \int dx$). For the corner term, we also find

$$
I_c = \frac{2V_x}{\kappa}\left(\frac{\pi/2 - \arctan\dot{\rho}(t_f)}{z_f} + \frac{\pi/2 + \arctan\dot{\rho}(t_i)}{z_i}\right). \qquad (7)
$$

Integrating by parts, this action can be written only using first derivatives of ρ, yielding

$$
I = \frac{2V_x}{\kappa}\int_{t_i}^{t_f} dt\ \boxed{\left(\frac{1}{\rho^2} + \frac{\dot{\rho}\arctan\dot{\rho}}{\rho^2}\right)} + \cancel{\frac{\pi V_x}{\kappa}\left(\frac{1}{z_f}+\frac{1}{z_i}\right)}. \qquad (8)
$$

Simple example - eoms

The equations of motion obtained by extremizing (8) read

$$\boxed{\frac{\rho\ddot{\rho} + (1 + \dot{\rho}^2)}{\rho^3(1 + \dot{\rho}^2)^2} = 0.} \tag{9}$$

The generic solution to (30) reads

$$\rho(t) = \sqrt{\mathfrak{R}^2 - (t - t_0)^2} \tag{10}$$

and describes semi-circular arcs of radius $\mathfrak{R}$. The equal time slice $\dot{\rho} \to \infty$ corresponds to the limit of infinite radius.

Simple example - on-shell action

With boundary being $\rho(t_f) = z_f$ and $\rho(t_i) = z_i$, the value of the Euclidean action in the first term of (8) is

$$I = \frac{2V_x}{\kappa}\left(\frac{1}{z_f}\arctan\frac{z_i^2 - z_f^2 + \Delta t^2}{2z_f\Delta t} - \frac{1}{z_i}\arctan\frac{z_i^2 - z_f^2 - \Delta t^2}{2z_i\Delta t}\right). \qquad (11)$$

Now extremising w.r.t. Δt (keeping $z_i \neq z_f$ fixed) gives $\Delta t = 0$, i.e. $\mathfrak{R} \to \infty$, and

$$I_{min} = \frac{c\pi V_x}{24}\left(\frac{1}{z_f} - \frac{1}{z_i}\right). \qquad (12)$$

→ We recover the complexity=volume proposal?!

Simple example - comparison to Liouville

For $\dot{\rho} \ll 1$,

$$I = \frac{2V_x}{\kappa} \int_{t_i}^{t_f} dt \left(\frac{1}{\rho^2} + \frac{\dot{\rho} \arctan \dot{\rho}}{\rho^2} \right) \approx \frac{2V_x}{\kappa} \int dt \left(\frac{1}{\rho^2} + \frac{\dot{\rho}^2}{\rho^2} \right), \quad (13)$$

which, assuming no x-dependence, is equivalent to the Liouville Lagrangian

$$S_L = \frac{c}{24\pi} \int dt \int dx \left(\eta \, e^{2\omega} + (\partial_t \omega)^2 + (\partial_x \omega)^2 \right). \quad (14)$$

after a change of variables $\rho(t) \to (1/\sqrt{\eta}) \, e^{-\omega(t)}$. The equations of motion derived from (13) take the form

$$\boxed{\frac{\rho \ddot{\rho} + (1 - \dot{\rho}^2)}{\rho^3} = 0.} \quad (15)$$

Comparison to Boruch et al.

Note that [Boruch et al. 2021b] investigates a setup similar to us, and up to notation (6) also appears in the appendix of that paper. Following [Boruch et al. 2021b], we introduce a conformal time u, with

$$du = \sqrt{1 + \dot{\rho}(t)^2} dt, \tag{16}$$

such that the line element (3) is transformed into the conformal gauge form

$$ds^2 = \frac{du^2 + dx^2}{\varrho(u)^2}. \tag{17}$$

with the new $\varrho(u(t)) = \rho(t)$. The action now reads [Boruch et al. 2021b]

$$I = \frac{2V_x}{\kappa} \int_{u_i[\varrho]}^{u_f[\varrho]} du \left(\frac{\sqrt{1 - \varrho'^2} + \varrho' \arcsin \varrho'}{\varrho^2} \right) . \tag{18}$$

Comparison to Boruch et al.

From this, [Boruch et al. 2021b] obtains eoms

$$\frac{\varrho\varrho'' + 2(1-\varrho'^2)}{\varrho^3(1-\varrho'^2)^2} = 0, \tag{19}$$

which are *inequivalent* to our eoms, which in terms of ϱ and u take the Liouville form:

$$\frac{\varrho\varrho'' + (1-\varrho'^2)}{\varrho^3} = 0. \tag{20}$$

Problem: Integral $\int_{u_i[\varrho]}^{u_f[\varrho]} du$ has ρ-dependent boundary conditions!

→ [Boruch et al. 2021b] and [Chandra et al. 2021] study *different variational problems*!

Kinematic space

Kinematic space approach

Let us analyse the same problem from a kinematic space [Czech et al. 2015] point of view:

At each point $(z = \rho(t), t, 0)$, there is a geodesic (with endpoints at $(t_1(t), t_2(t))$) tangent to the cutoff surface. We find:

$$t_{1,2}(t) = t + \rho\dot{\rho} \pm \rho\sqrt{\dot{\rho}^2 + 1}. \quad (21)$$

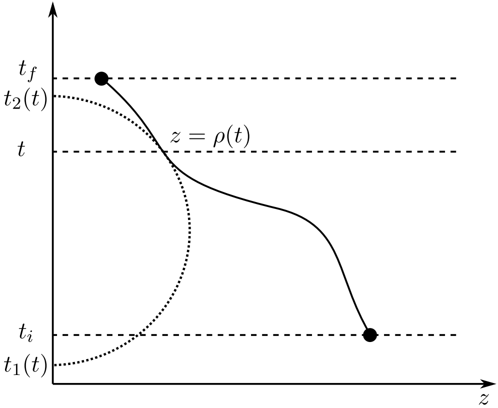

Kinematic space approach

Kinematic space (for $x = const.$ slice):

$$ds_{ks}^2 = \frac{-dt_1\, dt_2}{(t_1 - t_2)^2}. \tag{22}$$

Consider now the action

$$S_{ks} \sim \int \frac{dx}{\rho} ds_{ks}(t), \tag{23}$$

with the coordinate x in units of the cutoff ρ. This results in

$$S_{ks} \sim \int dt dx \left| \frac{\rho\ddot{\rho} + (1 + \dot{\rho}^2)}{\rho^2(1 + \dot{\rho}^2)} \right|, \tag{24}$$

which agrees with the bulk action in the form (6) as long as $\rho\ddot{\rho} \geq -(1 + \dot{\rho}^2)$ (path in kinematic space is timelike!).

For the solutions of (30), (24) vanishes identically!

Generic flow equations

Generic Flow Equations

We use the ADM formalism [Arnowitt et al. 1962] to write the metric as

$$ds^2 = N^2 dr^2 + g_{mn}(x,r)(dx^m + N^m dr)(dx^n + N^n dr) \tag{25}$$

and the Lagrangian in terms of canonical variables

$$\mathcal{L} = \sqrt{g}\,(\pi^{mn}\partial_r g_{mn} - NH - N^m H_m)\,, \tag{26}$$

$$\pi_{mn} = -(K_{mn} - K g_{mn}) \tag{27}$$

where the lapse and shift functions appear as Lagrange multipliers enforcing

$$H = H^m = 0. \tag{28}$$

Generic Flow Equations

To describe the flow we imagine starting with a surface at constant r and moving the cutoff slightly so that $r \to r + \epsilon(x)$. Then

$$\delta_\epsilon S = 2 \int \sqrt{g}\epsilon(x) \left(K^{mn} K_{mn} - K^2 \right) , \tag{29}$$

We hence obtain the *flow equations*

$$K^n_m K^m_n - K^2 = 0. \tag{30}$$

What does $K^n_m K^m_n - K^2 = 0$ mean?

Equation of Motion

Our considerations in [Chandra et al. 2021] [Chandra et al. 2023] led us to study co-dimension one surfaces Q embedded into AdS according to the equation

$$K^n_m K^m_n - K^2 = 0. \qquad (30)$$

Notation [Poisson 2004]:

- $m, n, ...$: indices for surface coordinates y^m; $\mu, \nu, ...$: indices for ambient space coordinates x^μ.
- $e^\alpha_a = \partial x^\alpha / \partial y^a$: projectors to surface tangent space; n^α: normal vector
- g_{mn}: induced metric; $G_{\mu\nu}$: bulk metric.
- K_{mn}: extrinsic curvature tensor of the surface; $K = K^n_n$.
- $\mathcal{R}$: ambient space (bulk) curvature; R: induced curvature etc.

Equation of Motion

Our considerations in [Chandra et al. 2021] [Chandra et al. 2023] led us to study co-dimension one surfaces Q embedded into AdS according to the equation

$$K^n_m K^m_n - K^2 = 0. \tag{30}$$

Brute force ansatz:

- Define embedding $z = f(t, x)$.
- Calculate $K_{ij}[f, f', f'', \dot{f}, ...]$.
- Solve (30) as nonlinear PDE for f
- Problem is only tractable in particularly simple/symmetric setups. See [Chandra et al. 2021].

Equation of Motion

Our considerations in [Chandra et al. 2021] [Chandra et al. 2023] led us to study co-dimension one surfaces Q embedded into AdS according to the equation

$$K_m^n K_n^m - K^2 = 0. \tag{30}$$

Motivation 1:

- Is there a more elegant approach?
- E.g., (30) is matrix equation for K_m^n.
- Given a solution K_m^n, can we find corresponding embedding?
- Similar approach in [Fonda et al. 2017] to holo. EE. in higher curvature theories.

Equation of Motion

Our considerations in [Chandra et al. 2021] [Chandra et al. 2023] led us to study co-dimension one surfaces Q embedded into AdS according to the equation

$$K^n_m K^m_n - K^2 = 0. \tag{30}$$

Motivation 2:

In vacuum, due to the Hamiltonian constraint

$$0 \equiv H = R - 2\Lambda - \left(K^n_m K^m_n - K^2\right), \tag{31}$$

equation (30) demands that the Ricci curvature R of the induced metric of the surface is constant. Specifically, for $d = 3$ and AdS-radius $\Lambda = -1$, then $\mathcal{R} = -6$ and $R = -2$ → looking for *constant curvature surfaces*.

Darboux's observation

As pointed out in [Barbot et al. 2011], the French mathematician Darboux once remarked that:

> *It can be said that the total curvature has more importance in Geometry; as it depends only on the line element, it comes into play in all questions concerning the deformation of surfaces. In mathematical physics, on the contrary, it is the mean curvature [i.e. extrinsic curvature] which seems to play the dominant role* [Darboux 1889].

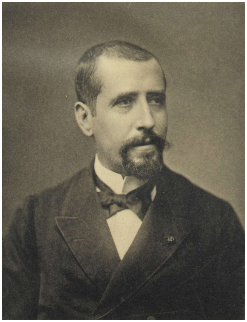

Jean-Gaston Darboux
1842 – 1917

Darboux's observation

More than 130 years later, Darboux's observation still seems to hold true, at least in AdS/CFT!

- The Ryu-Takayanagi formula [Ryu and Takayanagi 2006] demonstrates the role of surfaces with *constant (vanishing) extrinsic curvature* in the holographic dictionary.
- *"Darboux's question"* in AdS/CFT:
  Do surfaces of *constant intrinsic curvature* have a role in AdS/CFT, and if yes, which one?

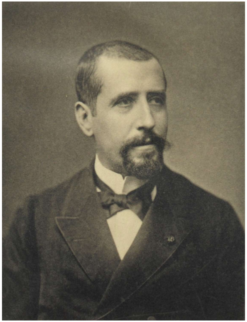

Jean-Gaston Darboux
1842 – 1917

Solving the equations of motion

Equations of motion:

$$K_m^n K_n^m - K^2 = 0 \tag{30}$$

$$\Leftrightarrow$$

$$R = 2\Lambda \text{ (in vacuum)} \tag{32}$$

$$\Leftrightarrow$$

$$\det K_{mn} = 0 \text{ (in } d_{induced} = 2) \tag{33}$$

Ansatz:

$$K_{mn} \equiv m_m m_n k \tag{34}$$

(generic in $d_{induced} = 2$, subset of solutions in $d_{induced} > 2$)

Solving the equations of motion

Codazzi equations [Poisson 2004]:

$$\mathcal{R}_{\alpha\beta\gamma\delta} e^\alpha_a e^\beta_b e^\gamma_c e^\delta_d = R_{abcd} \pm (K_{ad}K_{bc} - K_{ac}K_{bd}) \quad (35)$$

$$\mathcal{R}_{\mu\beta\gamma\delta} n^\mu e^\beta_b e^\gamma_c e^\delta_d = K_{bc|d} - K_{bd|c} \quad (36)$$

$$\left(\mathcal{R}_{\alpha\beta} - \frac{1}{2}\mathcal{R}G_{\alpha\beta}\right) n^\beta e^\alpha_a = K^b_{a|b} - K_{,a} \quad (37)$$

($\mathcal{R} \sim$ ambient; $R \sim$ induced geometry; $e^\alpha_a \sim$ projectors; $n^\beta \sim$ normal)

Solving the equations of motion

Codazzi equations [Poisson 2004], using ansatz $K_{mn} \equiv m_m m_n k$:

$$\mathcal{R}_{\alpha\beta\gamma\delta} e^\alpha_a e^\beta_b e^\gamma_c e^\delta_d = R_{abcd} \pm (K_{ad}K_{bc} - K_{ac}K_{bd}) \tag{35}$$

$$\Rightarrow \mathcal{R}_{\alpha\beta\gamma\delta} e^\alpha_a e^\beta_b e^\gamma_c e^\delta_d = R_{abcd} \pm 0 \tag{38}$$

($\mathcal{R} \sim$ ambient; $R \sim$ induced geometry; $e^\alpha_a \sim$ projectors; $n^\beta \sim$ normal)

Hence if the ambient space is (locally) maximally symmetric

$$\mathcal{R}_{\alpha\beta\gamma\delta} = \frac{\mathcal{R}}{d(d-1)} \left(G_{\alpha\gamma}G_{\beta\delta} - G_{\alpha\delta}G_{\beta\gamma}\right), \tag{39}$$

then so is the induced metric of the surface with $R = \frac{d-2}{d}\mathcal{R}$.

Solving the equations of motion

Furthermore, $G_{\alpha\beta}n^{\beta}e^{\alpha}_{a} = 0$ (ambient space is locally AdS), and (setting $k = \pm 1$, m_n unnormalised) we find:

$$\mathcal{R}_{\mu\beta\gamma\delta}n^{\mu}e^{\beta}_{b}e^{\gamma}_{c}e^{\delta}_{d} = K_{bc|d} - K_{bd|c} \tag{36}$$

$$\Rightarrow \quad 0 = m_c\nabla_d m_b + m_b\nabla_d m_c - m_d\nabla_c m_b - m_b\nabla_c m_d. \tag{40}$$

Now, set $d = 3$ and introduce $l^a m_a = 0, l^a l_a = const.$ Thus:

$$0 = m_d l^c l^b \nabla_c m_b \Rightarrow 0 = l^c l^b \nabla_c m_b. \tag{41}$$

$$l^b m_b = 0 \Rightarrow 0 = l^c\nabla_c(l^b m_b) = (l^c\nabla_c l^b)\, m_b + \underbrace{l^c l^b \nabla_c m_b}_{=0}. \tag{42}$$

Also, $(l^c\nabla_c l^b)\, l_b \propto l^c\nabla_c l^b l_b = 0$ and hence $l^c\nabla_c l^b = 0$ – geodesic equation.

Solving the equations of motion

Recall:

$$l^a m_a = 0 \Rightarrow K_{ab} l^a l^b = 0 \tag{43}$$

The relation between the covariant derivative in the ambient space $X_{;\beta}$ and the covariant derivative in the induced metric $X_{|b}$ gives [Poisson 2004]

$$l^\alpha_{;\beta} e^\beta_b = l^a_{|b} e^\alpha_a \pm l^a K_{ab} n^\alpha. \tag{44}$$

Contracting (44) with l^b, we find

$$\underbrace{l^\beta l^\alpha_{;\beta}}_{\text{ambient space geodesic eq.}} = \underbrace{l^b l^a_{|b}}_{\text{induced metric geodesic eq.}} e^\alpha_a \pm l^b l^a K_{ab} n^\alpha. \tag{45}$$

The surface is foliated by curves which are geodesics in the ambient space.

Solving the equations of motion

The surface with $R = -2$ is foliated by curves which are geodesics in the ambient space (with $\mathcal{R} = -6$).

Analogue statement in $\mathbb{R}^3$:
All developable surfaces (i.e. $R = 0$) are ruled surfaces (i.e. foliated by straight lines) [Krivoshapko and Ivanov 2015], however the converse is not true.

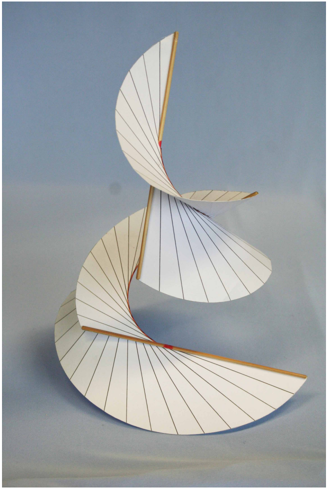

Example 1: Euclidean AdS_3, Poincaré-patch

Background:

$$ds^2 = \frac{1}{z^2}\left(dt^2 + dx^2 + dz^2\right) \tag{46}$$

Solution for strip of varying width:

$$z(t,x) = \sqrt{r(t)^2 - x^2}, \tag{47}$$

Genralizes case of constant width studied in [Chandra et al. 2021].

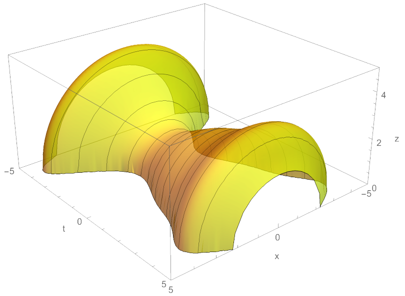

Example 2: Uniqueness?

Background:

$$ds^2 = \frac{1}{z^2}\left(dt^2 + dx^2 + dz^2\right) \tag{48}$$

For elliptic boundary region, there are two hypersurfaces satisfying (30) with the same boundary condition at $z = 0$. For one we find $K < 0$ everywhere, while for the other one we find $K > 0$ everywhere.

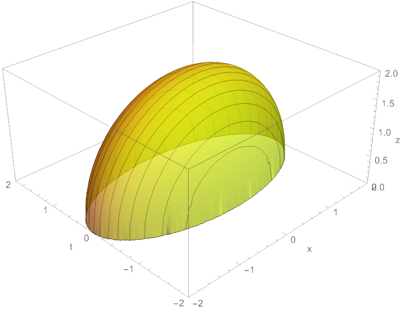

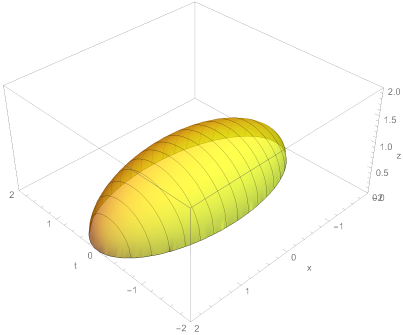

Example 3: Lorentzian (global) AdS_3, specelike surfaces

Background:

$$ds^2 = \frac{1}{\cos(\theta)^2}\left(-dt^2 + d\theta^2 + \sin(\theta)^2 d\phi^2\right), \tag{49}$$

Solution:

$$t(\phi,\theta) = t_{bdy}\left[\arctan\left(\sqrt{\csc^2(\theta)\sec^2(\phi) - 1}\right)\right] \tag{50}$$

where $t_{bdy}[\phi]$ is the boundary condition at the asymptotic boundary $\theta = \pi/2$ which we assume to be symmetric under $\phi \to -\phi$.

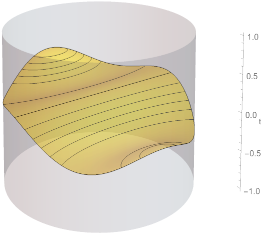

Example 4: "Lemons"

Let's now search for timelike surfaces in Lorentzian AdS.

Timelike oscillating geodesic:

$$t(\theta) = \pm \arctan\left(\frac{E\sin(\theta)}{\sqrt{-1+E^2\cos(\theta)^2}}\right), \quad \phi = const. \tag{51}$$

where the "energy" $E > 1$ of the geodesic is related to its turning point θ_{max} by $\theta_{max} = \arccos 1/E$. we can construct surfaces of the form

$$t(\theta,\phi) = \pm \arctan\left(\frac{E(\phi)\sin(\theta)}{\sqrt{-1+E(\phi)^2\cos(\theta)^2}}\right) + const. \tag{52}$$

where we have promoted E to a ϕ-dependent parameter.
K diverges at $\theta = 0$ where the surfaces will have a conical singularity.

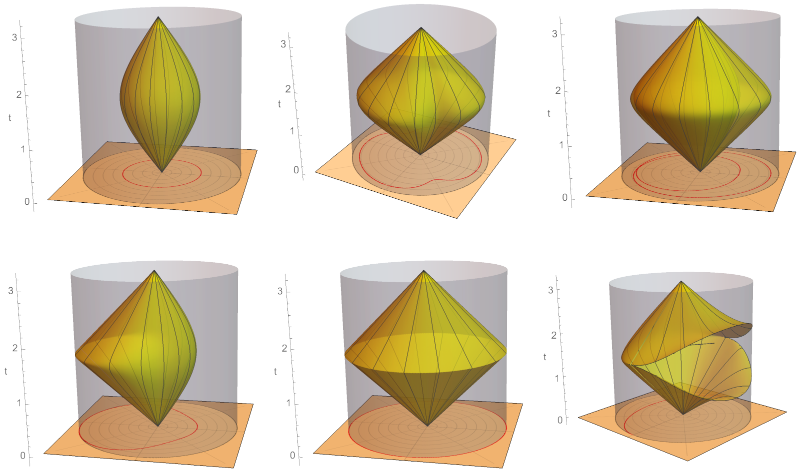

From top-left to bottom-right: $E(\phi) = \sqrt{2}$, $E(\phi) = 2\sin(2\phi) + \cos(4\phi) + 5$, $E(\phi) = 5\sin^2\left(\frac{\phi}{4}\right) + \sqrt{2}$, $E(\phi) = \tan^4\left(\frac{\phi}{2}\right) + \sqrt{2}$, $E \to \infty$, and

$E(\phi) = \left(\frac{\cos(\phi)}{\sin(\phi)}\right)^2 + 2$ for $0 < \phi < \pi$, $E(\phi) = -i\left(\left(\frac{\cos(\phi)}{\sin(\phi)}\right)^2 + 2\right)$ for $\pi < \phi < 2\pi$.

Lemons, Observations:

- All lemons have "height" $\Delta t = \pi$.
- Action inside finite Lemons is $I_{EH} + I_{GHY} = 4\pi^2$, independent of E by construction: These surfaces bound regions of the bulk whose action does not change under infinitesimal deformations of their boundary.
- Imaginary values of $E(\phi)$ lead to spacelike surfaces that reach the boundary.
- $t(\theta, \phi) = \theta$, for $E \to \infty$; surface becomes *null boundary of WDW patch*.

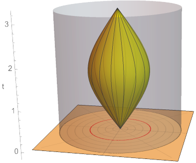

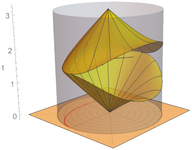

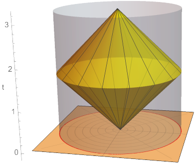

Lemons, Questions/Speculations:

- All lemons have "height" $\Delta t = \pi$.
  $\rightarrow$ Is there a specific $T\bar{T}$ deformation that describes a theory living on this surface?

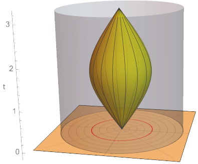

- Action inside finite Lemons is
  $I_{EH} + I_{GHY} = 4\pi^2$, independent of E.
- Imaginary values of $E(\phi)$ lead to spacelike surfaces that reach the boundary.
  $\rightarrow$ Complexify coordinates?

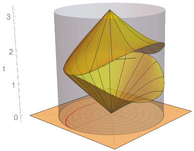

- $t(\theta, \phi) = \theta$, for $E \rightarrow \infty$; surface becomes null boundary of WDW patch.
  $\rightarrow$ Value of action in this limit?
  $\rightarrow$ $E \gg 1$ as regularisation of WdW-patch?
  $\rightarrow$ WdW patch arises naturally, without "infinite tension" limit of [Boruch et al. 2021a].

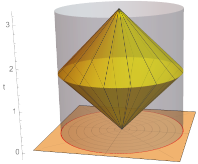

Kinematic space connection?

The solutions to the flow equation

$$K^n_m K^m_n - K^2 = 0. \qquad (30)$$

are foliated by geodesics of the ambient space.

That means: these surfaces are described by *curves in the space of geodesics* (∼kinematic space [Czech et al. 2015], generalised in [Czech et al. 2016] [Czech et al. 2020] [Chagnet et al. 2022]).

⇒ Can we phrase our results from a kinematic space perspective?

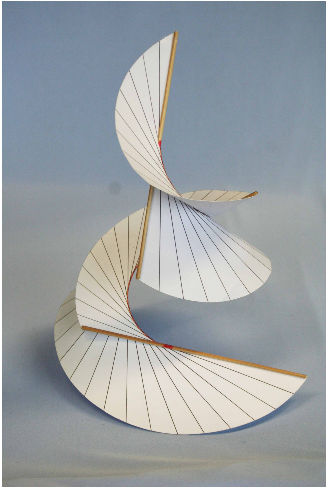

Summary

Summary and outlook

- Groundwork laid in [Caputa et al. 2017a] [Caputa et al. 2017b] [Boruch et al. 2021b] with *path integral optimization*.
- In simple Euclidean case, extremising action under a dynamic cutoff surface reproduces equal time slice/CV proposal [Chandra et al. 2021].
- Generalisation to Lorentzian case is non-trivial, with many challenges (e.g. boundedness of action) [Chandra et al. 2023].
- Universal flow equation derived in [Chandra et al. 2021] can be solved quite generally → suggests konnection to kinematic space.
- See also next talk by Andrew!


Thank you very much
for your attention


Back-up slides...

Gauss-Bonnet theorem

Implications of the Gauss-Bonnet theorem

Consider the Gauss-Bonnet theorem [Troyanov 1991]

$$\int_Q \frac{R}{2} dV + \int_{\partial Q} k_g ds + \sum_{\text{corners } c} \alpha_c + \sum_{\text{conical sing. } s} \beta_s = 2\pi\chi, \tag{53}$$

As we are searching for $2d$ surfaces of constant scalar curvature, we find

$$\int_Q \frac{R}{2} dV = \frac{R}{2} V < 0 \tag{54}$$

So for $\chi \geq 0$ (includes all Lorentzian cases), surface either needs to reach boundary *or* have conical singularities!

Conical singularities in the Gauss-Bonnet formula

In order to derive the contribution of conical singularities, we start with

$$\int_Q \frac{R}{2} dV + \int_{\partial Q} k_g ds + \sum_{\text{(old) corners } c} \alpha_c + X_{\text{conical sing.}} = 2\pi\chi. \tag{55}$$

We resolve the singularity by introducing a cut:

$$\int_Q \frac{R}{2} dV + \int_{\partial Q} k_g ds + \sum_{\text{(old) corners } c} \alpha_c + \sum_{\text{new corners } c} \alpha_c = 2\pi(\chi - 1). \tag{56}$$

Comparing (55) and (56), we find

$$X_{\text{conical sing.}} = \sum_{\text{new corners } c} \alpha_c + 2\pi = \alpha_{c1} + \alpha_{c2} + 2\pi = \delta. \tag{57}$$

with $\alpha_{c1} = -\pi$. $\alpha_{c2} = -(\pi - \delta)$, and deficit angle δ.

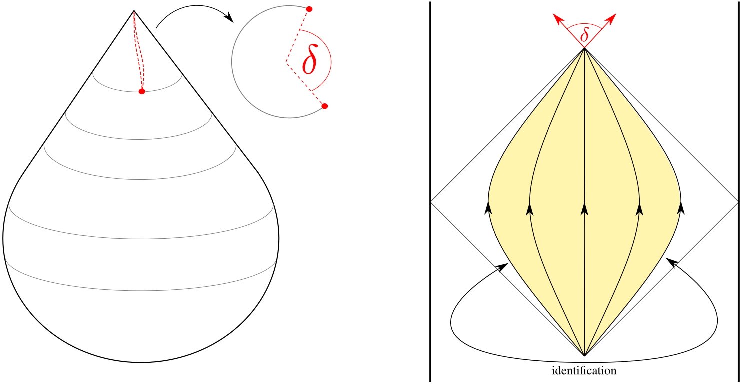

Left: Introducing a cut to derive contribution from conical singularities in Euclidean case.

Right: Lorentzian deficit angle for lemon surface.

Lorentzian case

For the Lorentzian Gauss-Bonnet theorem, see e.g. [Helzer 1974]. One has to define the (always real valued) oriented *Lorentzian angle* δ between two future pointing normalised timelike vectors X and Y to satisfy

$$\cosh(\delta) = -X \cdot Y. \tag{58}$$

The Lorentzian Gauss-Bonnet-theorem then takes the form

$$\int_Q \frac{R}{2} dV + \int_{\partial Q} k_g ds + \sum_{\text{corners } c} \alpha_c + \sum_{\text{conical sing. } s} \beta_s = 0, \tag{59}$$

Firstly, the right hand side automatically vanishes ($\chi \equiv 0$), secondly, traversing a closed timelike geodesic polygon in flat space yields the total Lorentzian angle

$$\alpha_{12} + \alpha_{23} + ... + \alpha_{n1} = 0. \tag{60}$$

Application to Lemons

Assume E indep. of ϕ. Induced metric:

$$ds^2 = \frac{1}{\cos(\theta_2)^2}\left(-dt_2^2 + d\theta_2^2\right), \tag{61}$$

with

$$4\text{arctanh}\left(\tan\left(\frac{\theta_{max,2}}{2}\right)\right) = 2\pi\tan(\theta_{max,3}). \tag{62}$$

Hence:

$$\frac{RV}{2} = -4\pi\tan(\theta_{max,3}) = -4\pi\sqrt{E^2 - 1}. \tag{63}$$

Application to Lemons

$$\frac{RV}{2} = -4\pi \tan(\theta_{max,3}) = -4\pi \sqrt{E^2 - 1}. \tag{63}$$

Tangent vectors of boundary geodesics:

$$X_{\pm}^{m} = \begin{pmatrix} X_{\pm}^{t_2} \\ X_{\pm}^{\theta_2} \end{pmatrix} = \begin{pmatrix} E_2 \\ \pm\sqrt{E_2^2 - 1} \end{pmatrix} \tag{64}$$

Hence:

$$\delta_{\text{future conical sing.}} = \text{arccosh}\left(-X_+ \cdot X_-\right) = 2\pi \tan(\theta_{max,3}) \tag{65}$$

$$= \delta_{\text{past conical sing.}} \tag{66}$$

Gaus-Bonnet theorem

$$\frac{RV}{2} + \delta_{\text{past conical sing.}} + \delta_{\text{future conical sing.}} = 0. \tag{67}$$

is satisfied.

Lemons in higher dimensions

"Lemons" in higher dimensions

Let's consider global Lorentzian AdS_4,

$$ds^2 = \frac{1}{\cos(\theta)^2}\left(-dt^2 + d\theta^2 + \sin(\theta)^2 d\psi^2 + \sin(\theta)^2 \sin(\psi)^2 d\phi^2\right), \tag{68}$$

(boundary at $\theta = \pi/2$) and assume rotational symmetry. Ansatz:

$$t(\theta, \psi, \phi) = f(\theta). \tag{69}$$

Equation (30) then yields the ODE

$$4\cot(\theta) f'(\theta) f''(\theta) - 2\left(\csc^2(\theta) + 2\right) f'(\theta)^2 \left(f'(\theta)^2 - 1\right) = 0, \tag{70}$$

$$\Rightarrow f'(\theta) = \pm \frac{\sqrt{\sin(2\theta)}\cot(\theta)}{\sqrt{\mathrm{C} + \sin(2\theta)\cot^2(\theta)}} \tag{71}$$

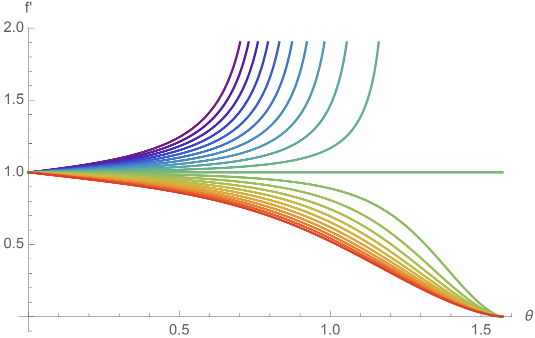

$f'(\theta) = +\frac{\sqrt{\sin(2\theta)}\cot(\theta)}{\sqrt{\mathrm{C}+\sin(2\theta)\cot^2(\theta)}}$ for C between -1 (blue) and 1 (red). AdS_4 boundary is at $\theta = \pi/2$.

- $C = 0 \Rightarrow f' = 1 \Rightarrow$ null boundary of the WDW patch.
- $C > 0 \Rightarrow f' \leq 1 \Rightarrow$ spacelike surface reaching to the boundary.
- $C < 0 \Rightarrow f' \geq 1 \Rightarrow$ Lemon like surface which turns around at finite $\theta_{max} \leq \pi/2$.

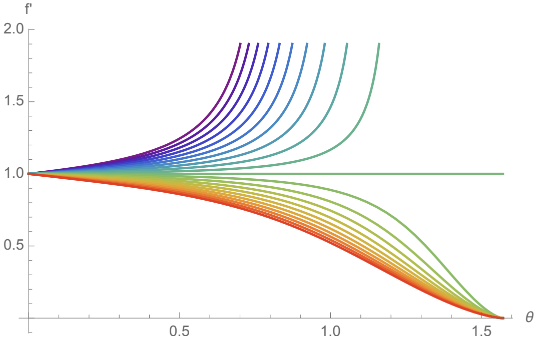

$f'(\theta) = +\frac{\sqrt{\sin(2\theta)}\cot(\theta)}{\sqrt{C+\sin(2\theta)\cot^2(\theta)}}$ for C between -1 (blue) and 1 (red). AdS_4 boundary is at $\theta = \pi/2$.

Differences and similarities to $d = 3$:

- $K_{mn} \neq m_m m_n k$
- $f'(0) = 1$ for any C, hence induced metric ($\neq AdS_3$) is degenerate at tip; curvature singularity in Kretschmann scalar.
- "Height" (time-span) of $AdS_{d\geq 4}$ lemons depends on C ($\sim$ turning point).

References

R. Arnowitt, S. Deser, and W. Misner. The dynamics of General Relativity. In L. Witten, editor, *Gravitation: an introduction to current research*, chapter 7, pages 227–265. Wiley, New York, 1962. doi: 10.1007/s10714-008-0661-1.

T. Barbot, F. Béguin, and A. Zeghib. Prescribing Gauss curvature of surfaces in 3-dimensional spacetimes Application to the Minkowski problem in the Minkowski space. *Annales de l'Institut Fourier*, 61(2):511–591, 2011. doi: 10.5802/aif.2622. URL https://aif.centre-mersenne.org/articles/10.5802/aif.2622/.

J. Boruch, P. Caputa, D. Ge, and T. Takayanagi. Holographic path-integral optimization. *JHEP*, 07: 016, 2021a. doi: 10.1007/JHEP07(2021)016.

J. Boruch, P. Caputa, and T. Takayanagi. Path-Integral Optimization from Hartle-Hawking Wave Function. *Phys. Rev. D*, 103(4):046017, 2021b. doi: 10.1103/PhysRevD.103.046017.

H. A. Camargo, P. Caputa, and P. Nandy. Q-curvature and Path Integral Complexity. 1 2022.

P. Caputa, N. Kundu, M. Miyaji, T. Takayanagi, and K. Watanabe. Anti-de Sitter Space from Optimization of Path Integrals in Conformal Field Theories. *Phys. Rev. Lett.*, 119(7):071602, 2017a. doi: 10.1103/PhysRevLett.119.071602.

P. Caputa, N. Kundu, M. Miyaji, T. Takayanagi, and K. Watanabe. Liouville Action as Path-Integral Complexity: From Continuous Tensor Networks to AdS/CFT. *JHEP*, 11:097, 2017b. doi: 10.1007/JHEP11(2017)097.

P. Caputa, D. Das, and S. R. Das. Path integral complexity and Kasner singularities. *JHEP*, 01:150, 2022. doi: 10.1007/JHEP01(2022)150.

N. Chagnet, S. Chapman, J. de Boer, and C. Zukowski. Complexity for Conformal Field Theories in General Dimensions. *Phys. Rev. Lett.*, 128(5):051601, 2022. doi: 10.1103/PhysRevLett.128.051601.

A. R. Chandra, J. de Boer, M. Flory, M. P. Heller, S. Hoertner, and A. Rolph. Spacetime as a quantum circuit. *JHEP*, 04:207, 2021. doi: 10.1007/JHEP04(2021)207.

A. R. Chandra, J. de Boer, M. Flory, M. P. Heller, S. Hörtner, and A. Rolph. Cost of holographic path integrals. *SciPost Phys.*, 14:061, 2023. doi: 10.21468/SciPostPhys.14.4.061.

B. Czech, L. Lamprou, S. McCandlish, and J. Sully. Integral Geometry and Holography. *JHEP*, 10: 175, 2015. doi: 10.1007/JHEP10(2015)175.

B. Czech, L. Lamprou, S. McCandlish, B. Mosk, and J. Sully. A Stereoscopic Look into the Bulk. *JHEP*, 07:129, 2016. doi: 10.1007/JHEP07(2016)129.

B. Czech, Y. D. Olivas, and Z.-z. Wang. Holographic integral geometry with time dependence. *JHEP*, 12:063, 2020. doi: 10.1007/JHEP12(2020)063.

G. Darboux. *Leçons sur la theorie générale des surfaces et les applications géométriques du calcul infinitésimal: les congruences et les équations lineaires aux dérivées partielles, des lignes tracées sur les surfaces*. Number 2 in Cours de géométrie de la Faculté des Sciences. Gauthier Villars, 1889. URL https://books.google.es/books?id=dzteAAAAcAAJ.

P. Fonda, V. Jejjala, and A. Veliz-Osorio. On the Shape of Things: From holography to elastica. *Annals Phys.*, 385:358–398, 2017. doi: 10.1016/j.aop.2017.08.011.

J. Hartle and R. Sorkin. Boundary Terms in the Action for the Regge Calculus. *Gen. Rel. Grav.*, 13: 541–549, 1981. doi: 10.1007/BF00757240.

G. Hayward. Gravitational action for space-times with nonsmooth boundaries. *Phys. Rev. D*, 47: 3275–3280, 1993. doi: 10.1103/PhysRevD.47.3275.

G. Helzer. A relativistic version of the Gauss-Bonnet formula. *Journal of Differential Geometry*, 9(4):507 – 512, 1974. doi: 10.4310/jdg/1214432546. URL https://doi.org/10.4310/jdg/1214432546.

S. Krivoshapko and V. Ivanov. *Encyclopedia of Analytical Surfaces*. Springer International Publishing, 2015. ISBN 9783319117737. URL https://books.google.de/books?id=cXTdBgAAQBAJ.

E. Poisson. *A Relativist's Toolkit: The Mathematics of Black-Hole Mechanics*. Cambridge University Press, 2004. ISBN 9781139451994. URL https://books.google.es/books?id=bk2XEgz_ML4C.

S. Ryu and T. Takayanagi. Holographic derivation of entanglement entropy from AdS/CFT. *Phys. Rev. Lett.*, 96:181602, 2006. doi: 10.1103/PhysRevLett.96.181602.

M. Troyanov. Prescribing curvature on compact surfaces with conical singularities. *Transactions of the American Mathematical Society*, 324(2):793–821, 1991. ISSN 00029947. URL http://www.jstor.org/stable/2001742.